*Article*

MMS

Mathematics and Mechanics of Solids
1–12

DOI: 10.1177/1081286514555451
mms.sagepub.com

SAGE

# The near-resonant regimes of a moving load in a three-dimensional problem for a coated elastic half-space

**Bariş Erbaş**
*(Department of Mathematics,) Anadolu University, Eskişehir, Turkey*

**Julius Kaplunov**
*(School of Computing and Mathematics,) Keele University, Staffordshire, UK*

**Danila A Prikazchikov**
*(School of Computing and Mathematics,) Keele University, Staffordshire, UK*

**Onur Şahin**
*(Department of Mathematics,) Anadolu University, Eskişehir, Turkey*

Received 17 September 2014; accepted 20 September 2014

**Abstract**

This paper deals with the three-dimensional analysis of the near-resonant regimes of a point load, moving steadily along the surface of a coated elastic half-space. The approach developed relies on a specialized hyperbolic–elliptic formulation for the wave field, established earlier by the authors. Straightforward integral solutions of the two-dimensional perturbed wave equation describing wave propagation along the surface are derived along with their far-field asymptotic expansions obtained using the uniform stationary phase method. Both sub-Rayleigh and super-Rayleigh cases are studied. It is shown that the singularities arising at the contour of the Mach cones typical of the super-Rayleigh case, are smoothed due to the dispersive effect of the coating.

**Keywords**

3D elasticity, moving load, Rayleigh wave, thin coating, uniform asymptotics

## 1. Introduction

Various modern industrial applications, including the development of high-speed train operation, significantly enhance the importance of three-dimensional (3D) modeling of elastic structures under moving loads, see e.g. Cao et al. [1]. Moving load problems have been analyzed for more than a century, see Fryba [2] and references therein. Among the numerous publications on the subject, most contributions have been carried out within a two-dimensional (2D) framework. Very few analytical studies dealing with 3D problems have focussed

**Corresponding author:**
Julius Kaplunov, School of Computing and Mathematics, Keele University, Staffordshire, ST5 5BG, UK.
Email: j.kaplunov@keele.ac.uk

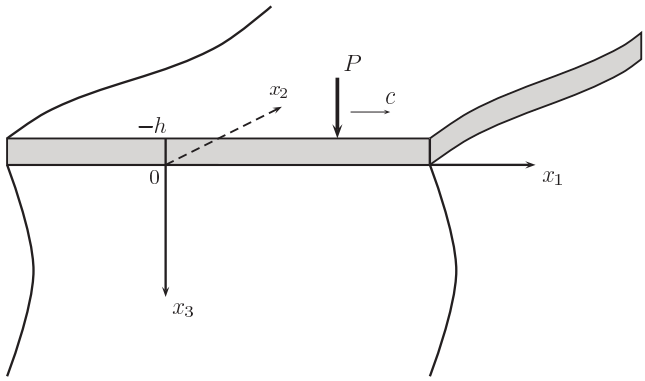


**Figure 1.** Coated half-space under a moving load.

on the numerical evaluation of exact solutions expressed in integral form. As an example, we mention the developments in Georgiadis and Lykotrafitis [3] using the Radon transform.

In this paper we adapt the asymptotic methodology that is based on extracting the contribution of the Rayleigh wave to the overall dynamic response. A specialized formulation for a near-surface wave field initially derived for the plane strain problem [4] was later generalized to the 3D setup taking into account the effect of a thin coating [5]. The cited papers develop a perturbation scheme starting from the presentation of the Rayleigh wave eigensolutions in terms of arbitrary harmonic functions, see Chadwick [6] and Kiselev and Parker [7]. In this case, the decay over the interior is governed by elliptic equations for elastic potentials, whereas surface wave propagation is described by a hyperbolic equation, which is singularly perturbed by a pseudo-differential operator in the presence of a coating. The hyperbolic-elliptic model developed has already been applied to a transient 2D moving load problem [8] providing drastic simplification to resonant analysis and enabling qualitative insight into transient dynamic phenomena. An explicit 3D steady-state solution for a moving load on an elastic half-space has also recently been obtained [9].

Below we consider the near-resonant regimes of a point load, steadily moving along the surface of a coated half-space. The previous considerations dealing with layered structures [10, 11] have had little focus on resonant phenomena. The 3D treatment presented extends the results of the above mentioned publication [9], and also a more recent paper [12], investigating a steady-state plane strain problem for a coated half-space. The problem studied has two small parameters, one of which is associated with the proximity of the speed of the moving load to the resonant Rayleigh wave speed, whereas another one originates from the small thickness of the coating. Scaling, incorporating the effect of both these parameters is determined. Analysis of the super-Rayleigh regime reveals Mach cones similar to those in the case of an uncoated half-space [9], which are now smoothed due to the dispersive effect of the coating. A relatively simple integral solution is subject to asymptotic analysis in the far-field using the uniform stationary phase method. The leading order asymptotic behavior is expressed in terms of the Fresnel functions. The implementation of the causality principle is also addressed in application to a dispersive surface wave. For the sub-Rayleigh regime we also develop a uniform asymptotic procedure resulting in the leading order asymptotic behavior given by the Airy function.

This paper is organized as follows. Section 2 contains a statement of the problem, followed by the proposed asymptotic scaling. The super-Rayleigh regime of the moving load is analyzed in Section 3, whereas the final Section 4 deals with the sub-Rayleigh mode. Numerical comparisons of exact and asymptotic results are presented for both cases.

## 2. Statement of the problem and scaling

Consider the 3D linear elastodynamics of a half-space ($-\infty < x_1, x_2 < \infty$, $0 \le x_3 < \infty$) coated by a thin layer ($-\infty < x_1, x_2 < \infty$, $-h \le x_3 \le 0$) under a concentrated vertical force of magnitude $P$ moving at a constant speed $c$ along the line $x_2 = 0$ of the surface $x_3 = -h$, see Figure 1.

We start from the approximate elliptic–hyperbolic formulation for the Rayleigh wave field in a coated half-space proposed in Dai et al. [5]. Within the latter, the decay over the interior of the half-space is described by

pseudo-static elliptic equations for elastic potentials

$$\frac{\partial^2\phi}{\partial x_3^2}+k_1^2\Delta_2\phi=0,\qquad \frac{\partial^2\psi_i}{\partial x_3^2}+k_2^2\Delta_2\phi=0,\qquad i=1,2 \tag{1}$$

where

$$\Delta_2=\frac{\partial^2}{\partial x_1^2}+\frac{\partial^2}{\partial x_2^2},\qquad k_i=\left(1-\frac{c_{\mathrm{R}}^2}{c_i^2}\right)^{1/2},$$

with $c_1$, $c_2$, and $c_{\mathrm{R}}$ denoting the longitudinal, shear, and Rayleigh wave speeds, respectively.

The displacement vector $\mathbf{u}=(u_1,u_2,u_3)$ is expressed through the potentials as

$$\mathbf{u}=\operatorname{grad}\phi+\operatorname{curl}\psi,\qquad \psi=(-\psi_2,\psi_1,0). \tag{2}$$

The wave propagation along the plane $x_3=0$ is governed by the singularly perturbed hyperbolic equation

$$\Delta_2\phi-\frac{1}{c_{\mathrm{R}}^2}\frac{\partial^2\phi}{\partial t^2}-bh\sqrt{-\Delta_2}\Delta_2\phi=AP\delta(x_1-ct)\delta(x_2), \tag{3}$$

and the relations

$$\frac{\partial\phi}{\partial x_i}=\frac{2}{1+k_2^2}\frac{\partial\psi_i}{\partial x_3},\qquad i=1,2. \tag{4}$$

Here $b$, and $A$ are constants, depending on the material parameters of the half-space and the coating, and $\sqrt{-\Delta_2}$ is a pseudo-differential operator, for more details see Dai et al. [5]. The sign of the coefficient $b$ is crucial for the type (max or min) of the phase speed at zero wave number, see Shuvalov and Every [13], and also Dai et al. [5].

The sought-for approximation of the Rayleigh wave field over the half-space follows from the solution of the formulated problem in equations (1), (3) and (4). The derivation is considerably simplified in the case of tangential displacements along the plane $x_3=0$, which are expressed from equations (2) and (4) as

$$u_i=\frac{c_{\mathrm{R}}^2}{2c_2^2}\frac{\partial\phi}{\partial x_i},\quad i=1,2. \tag{5}$$

Below we restrict ourselves to the steady-state regime. On introducing the moving coordinate $\lambda=x_1-ct$, we get from equation (3) for the sub-Rayleigh ($c<c_{\mathrm{R}}$) and super-Rayleigh ($c>c_{\mathrm{R}}$) cases

$$\frac{\partial^2\phi}{\partial x_2^2}+\varepsilon^2\frac{\partial^2\phi}{\partial\lambda^2}-bh\sqrt{-\left(\frac{\partial^2}{\partial x_2^2}+\frac{\partial^2}{\partial\lambda^2}\right)}\left(\frac{\partial^2\phi}{\partial x_2^2}+\frac{\partial^2\phi}{\partial\lambda^2}\right)=AP\delta(\lambda)\delta(x_2) \tag{6}$$

and

$$\frac{\partial^2\phi}{\partial x_2^2}-\varepsilon^2\frac{\partial^2\phi}{\partial\lambda^2}-bh\sqrt{-\left(\frac{\partial^2}{\partial x_2^2}+\frac{\partial^2}{\partial\lambda^2}\right)}\left(\frac{\partial^2\phi}{\partial x_2^2}+\frac{\partial^2\phi}{\partial\lambda^2}\right)=AP\delta(\lambda)\delta(x_2), \tag{7}$$

respectively, where

$$\varepsilon=\left|1-\frac{c^2}{c_R^2}\right|^{1/2}. \tag{8}$$

The adapted model is oriented to the analysis of a near-resonant response dominated by the Rayleigh wave contribution and is valid provided that $\varepsilon\ll 1$, see Kaplunov et al. [8, 9]. It also assumes that the thickness of the coating $h$ is small compared to a typical wavelength, see Dai et al. [5]. The presence of two small parameters in equations (6) and (7) leads to two different types of degeneration, at $\varepsilon=0$ and at $h=0$, corresponding to the critical speed of the load coinciding with the Rayleigh wave speed, and an uncoated half-space, respectively. This observation motivates the scaling

$$\lambda=\frac{\xi bh}{\varepsilon^2},\qquad x_2=\frac{\eta bh}{\varepsilon^3}, \tag{9}$$

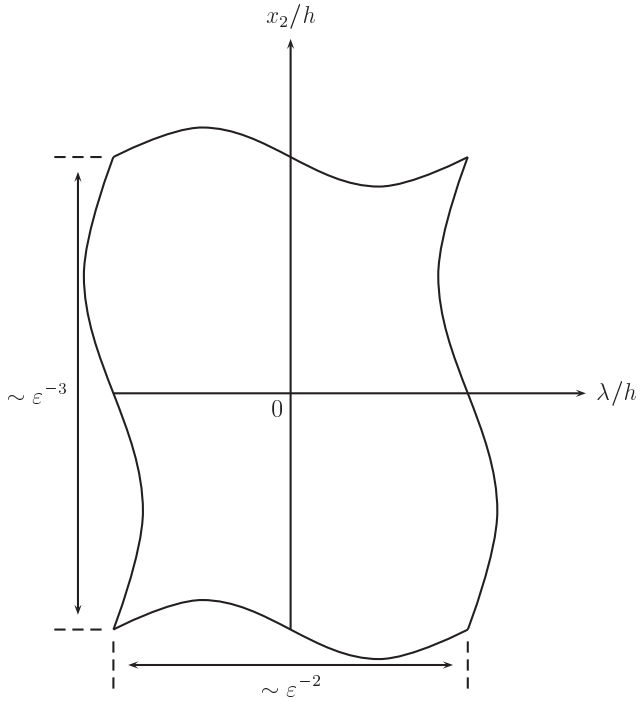


**Figure 2.** Asymptotic scaling.

which defines an elongated domain over the $\left(x_2 h^{-1}, \lambda h^{-1}\right)$ plane, see Figure 2. Using this scaling, equations (6) and (7) become

$$\frac{\partial^2 \phi}{\partial \eta^2} - \frac{\partial^2 \phi}{\partial \xi^2} - \sqrt{-\frac{\partial^2}{\partial \xi^2}}\,\frac{\partial^2 \phi}{\partial \xi^2} = \frac{AP}{\varepsilon}\delta(\xi)\,\delta(\eta) \tag{10}$$

and

$$\frac{\partial^2 \phi}{\partial \eta^2} + \frac{\partial^2 \phi}{\partial \xi^2} - \sqrt{-\frac{\partial^2}{\partial \xi^2}}\,\frac{\partial^2 \phi}{\partial \xi^2} = \frac{AP}{\varepsilon}\delta(\xi)\,\delta(\eta), \tag{11}$$

respectively.

## 3. The super-Rayleigh regime

Let us first study equation (10). On applying the Fourier transform in variable $\xi$, we obtain

$$\frac{\mathrm{d}^2 \phi^{\mathrm{F}}}{\mathrm{d}\eta^2} + k^2(1+|k|)\phi^{\mathrm{F}} = \frac{AP}{\varepsilon}\delta(\eta), \tag{12}$$

where

$$\phi^{\mathrm{F}}(k,\eta,0) = \int_{-\infty}^{\infty} \phi(\xi,\eta,0)\, e^{-ik\xi}\,\mathrm{d}\xi. \tag{13}$$

Bearing in mind the symmetry of the sought-for solution in $\eta$, we get

$$\phi^{\mathrm{F}} = \frac{AP}{\varepsilon}\frac{\sin\left(|k|\sqrt{1+|k|}|\eta|\right)}{|k|\sqrt{1+|k|}}. \tag{14}$$

The related inverse transform is given by

$$\phi(\xi,\eta,0)=\frac{AP}{\pi\varepsilon}\int\limits_0^\infty \frac{\sin\left(k\sqrt{1+k}|\eta|\right)\cos\left(k\xi\right)}{k\sqrt{1+k}}\,\mathrm{d}k. \tag{15}$$

The tangential displacements along the plane $x_3=0$ are expressed through the last integral by equation (5). The analysis is rather similar for both displacements, hence we deal with $u_1$ only. It can be written as

$$u_1(\xi,\eta,0)=\frac{APc_{\mathrm{R}}^2\varepsilon}{4\pi bhc_2^2}\sum_{n=1}^{2} I_n(\xi,\eta) \tag{16}$$

where

$$I_n(\xi,\eta)=\mathrm{sgn}(\xi)\int\limits_0^\infty \frac{\cos\left(|\xi|h_n(k)\right)}{g(k)}\,\mathrm{d}k, \qquad n=1,2, \tag{17}$$

with

$$g(k)=\sqrt{1+k}, \qquad h_n(k)=k\left[g(k)\mu-(-1)^n\right], \qquad \mu=\left|\frac{\eta}{\xi}\right|.$$

Let us investigate the far-field asymptotic behavior of the oscillating integrals (17) as $|\xi|\gg 1$, assuming $\mu\sim 1$. It may be shown that the effect of the first integral $I_1$ is asymptotically minor, whereas $I_2$ is dominated by the contribution of the stationary point of $h_2(k)$, given by

$$k_*=\frac{2\left(1-3\mu^2+\sqrt{3\mu^2+1}\right)}{9\mu^2}. \tag{18}$$

Note that at the contour of the Mach cone $\mu=1$ ($|\xi|=|\eta|$) the stationary point $k_*=0$ coincides with the lower limit of the integral $I_2$. Therefore, we have to apply the uniform stationary phase method, e.g. see Borovikov [14] and references therein, having at the leading order

$$I_2\sim \mathrm{Re}\left[\frac{e^{i|\xi|h_*}}{g_*}\int\limits_0^\infty e^{\frac{1}{2}i|\xi|h''(k_*)(k-k_*)^2}\mathrm{d}k\right], \tag{19}$$

where

$$h_*=h(k_*)=\frac{2\left(1-3\mu^2+\sqrt{3\mu^2+1}\right)\left(\sqrt{3\mu^2+1}-2\right)}{27\mu^2}, \tag{20}$$

and

$$g_*=g(k_*)=\frac{1+\sqrt{3\mu^2+1}}{3\mu}. \tag{21}$$

The resulting displacement $u_1$ is then given by

$$u_1\sim\frac{AP\varepsilon c_{\mathrm{R}}^2k_*}{4\pi bhc_2^2g_*a}\frac{\mathrm{sgn}(\xi)}{|\xi|^{1/2}}F(|\xi|,\mu), \tag{22}$$

where

$$F(|\xi|,\mu)=\cos\left[h_*|\xi|\right]\left\{\sqrt{\frac{\pi}{8}}-\mathrm{C}\left(a\sqrt{|\xi|}\right)\right\}-\sin\left[h_*|\xi|\right]\left\{\sqrt{\frac{\pi}{8}}-\mathrm{S}\left(a\sqrt{|\xi|}\right)\right\}, \tag{23}$$

with

$$a=-k_*\sqrt{\frac{h''(k_*)}{2}}=\frac{\left[3\mu^2-1-\sqrt{3\mu^2+1}\right]\sqrt[4]{3\mu^2+1}}{3\mu\left[1+\sqrt{3\mu^2+1}\right]}, \tag{24}$$

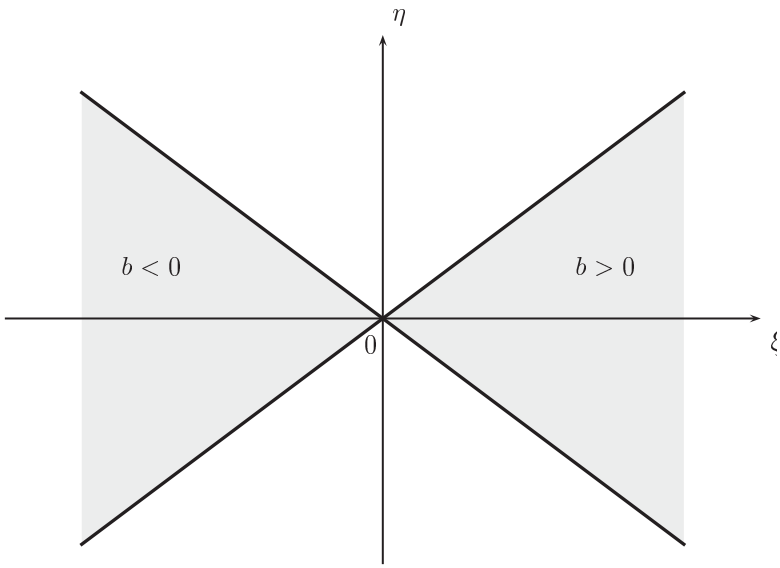


**Figure 3.** Mach cones.

and $S(x)$ and $C(x)$ are the Fresnel functions, defined by

$$S(x) = \int_0^x \sin(x^2)\,\mathrm{d}x, \qquad C(x) = \int_0^x \cos(x^2)\,\mathrm{d}x, \tag{25}$$

see e.g. Abramowitz and Stegun [15]. It is pretty obvious that the derived uniform asymptotic formula is also valid at $\mu > 1$ when $k_* < 0$ and $a$ takes imaginary values.

The interpretation of the formulae in this section written in terms of $|\xi|$ and $|\eta|$ relies on the implementation of the causality principle. In the absence of a coating, when $h = 0$, equation (10) degenerates to the wave equation. For the latter it is logical to deal with the Mach cones behind the load only, i.e. at $\xi > 0$ for $b > 0$ and $\xi < 0$ for $b < 0$, as follows from scaling (9), see Figure 3.

At the same time the full solution of the associated original problem in 3D elasticity will contain the contribution of faster compression and shear waves ignored within the framework of the adapted specialized formulation, see Section 1. As a result, the question of taking into consideration both Mach cones (behind and in front of the load) may be raised. To a certain extent, this may be relevant to the phenomenon of a head shear wave propagating faster than a cylindrical shear wave in the case of the plane Lamb problem, e.g. see Poruchikov [16].

Another interesting feature is concerned with the dispersive nature of the analyzed surface wave governed by a singularly perturbed wave equation. In this case, due to causality, we seemingly have to require decay of the solution outside the interior of the Mach cones predicted by the related degenerate non-dispersive equation. The asymptotic behavior of the Fresnel functions in equation (23) at the large imaginary values of the argument [15] show that the function (23) is exponentially small at $\mu - 1 \gg |\xi|^{-1}$.

Numerical illustrations of the scaled longitudinal displacement

$$U_1 = \frac{4\pi bhc_2^2}{APc_{\mathrm{R}}^2\varepsilon}u_1 \tag{26}$$

are presented in Figures 4 and 5, containing longitudinal and transverse cross-sections of the profile, respectively. On these plots, the results of the numerical integration of equation (16) are depicted by solid lines, with the dotted line corresponding to the asymptotic approximation (22). Figure 4 shows the dependence of $U_1$ on the transverse variable $|\eta|$, with calculations performed for the value of $|\xi| = 5$. Figure 5 mirrors Figure 4, depicting the variation of $U_1$ on $|\xi|$, with calculations performed for $|\eta| = 5$.

It can be clearly seen from both Figures 4 and 5, that the dispersive effect of the coating causes smoothing of the discontinuities along the lines $|\xi| = |\eta|$, arising in an uncoated half-space, see Kaplunov et al. [9]. The

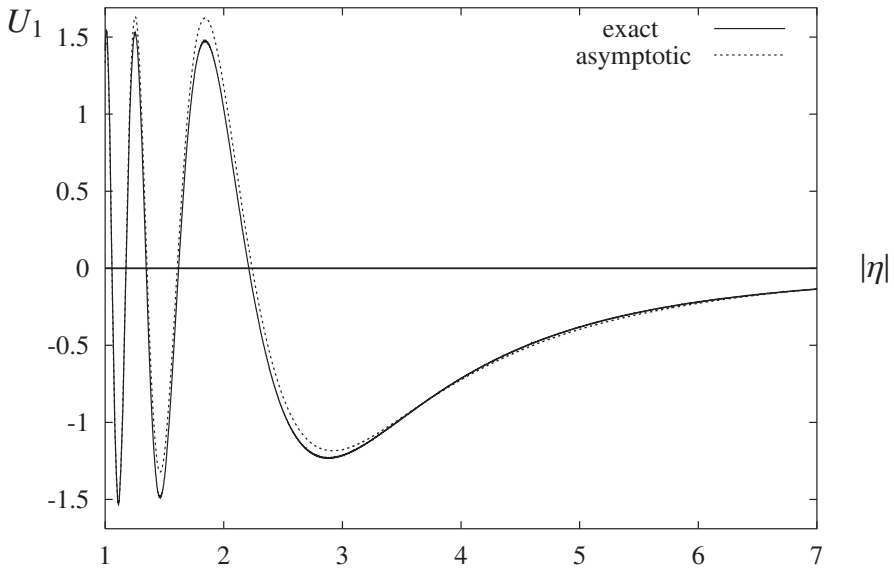


**Figure 4.** Profile of the super-Rayleigh displacement $U_1$ at $|\xi| = 5$.

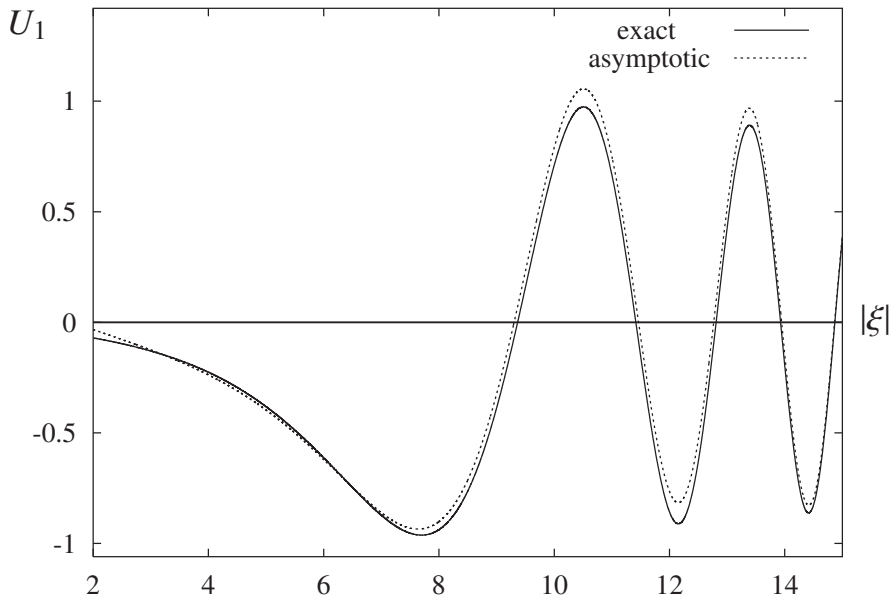


**Figure 5.** Profile of the super-Rayleigh displacement $U_1$ at $|\eta| = 5$.

oscillations occur within the Mach cone, decaying away from it. The periods of oscillation diminish on both graphs as $\mu \to 0$, due to $h_* \to \infty$, as may be noticed from equation (20).

The asymptotic formula (22) provides a surprisingly accurate approximation of the solution (16), which is applicable even at the not very large values of the parameter $|\xi|$, used on Figures 4 and 5. This is due to the argument of the Fresnel functions $a\sqrt{|\xi|} \sim |\xi|^{1/2}\mu^{-1}$ in equation (23), therefore we actually operate with a larger parameter $|\xi|\mu^{-2}$.

In order to provide a better overview of the investigated wave phenomena, we present a 3D illustration of a part of the scaled displacement profile, corresponding to the exact integral solution in equation (16), see Figure 6.

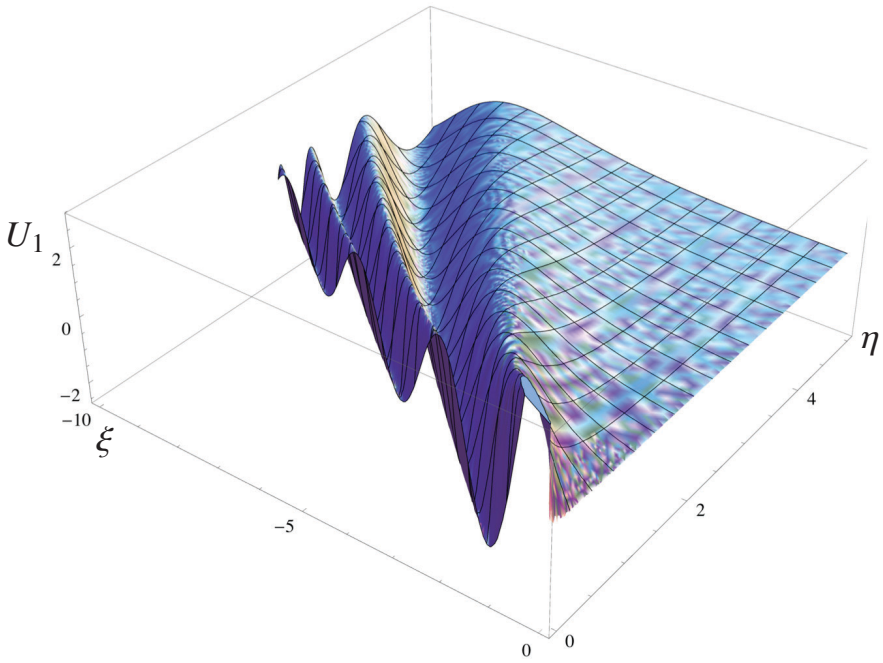


**Figure 6.** A 3D profile of the longitudinal super-Rayleigh displacement $U_1$.

## 4. The sub-Rayleigh regime

Let us now study equation (11). On applying the Fourier transform, we get

$$\frac{\mathrm{d}^2\phi^{\mathrm{F}}}{\mathrm{d}\eta^2} - k^2(1-|k|)\phi^{\mathrm{F}} = \frac{AP}{\varepsilon}\delta(\eta). \tag{27}$$

The solution of this equation is piecewise in the parameter $|k|$. Due to symmetry in $\eta$ along with decay at infinity, it may be written as

$$\phi^{\mathrm{F}}(k,\eta,0) = \begin{cases} -\dfrac{AP}{\varepsilon}\dfrac{e^{-|k|\sqrt{1-|k|}|\eta|}}{|k|\sqrt{1-|k|}}, & |k|<1; \\ \dfrac{AP}{\varepsilon}\dfrac{\sin\left(|k|\sqrt{|k|-1}|\eta|\right)}{|k|\sqrt{|k|-1}}, & |k|>1. \end{cases} \tag{28}$$

Then, we have for the longitudinal displacement along the plane, $x_3 = 0$

$$u_1(\xi,\eta,0) = \frac{AP\varepsilon c_{\mathrm{R}}^2 \mathrm{sgn}(\xi)}{2\pi c_2^2 bh}\left[\int_0^1 \frac{e^{-k\sqrt{1-k}|\xi|\mu}}{\sqrt{1-k}}\sin(k|\xi|)\,\mathrm{d}k - \int_1^\infty \frac{\sin\left(k\sqrt{k-1}|\xi|\mu\right)}{\sqrt{k-1}}\sin(k|\xi|)\,\mathrm{d}k\right]. \tag{29}$$

Consider the far-field approximation ($|\xi| \gg 1$). It can be verified that the leading order asymptotic behavior of $u_1$ is given by the contribution of the stationary points arising from the second integral in equation (29). Changing the variable $k$ to $t = \sqrt{k-1}$, this integral takes the form

$$\int_1^\infty \frac{\sin\left(k\sqrt{k-1}|\eta|\right)}{\sqrt{k-1}}\sin(k|\xi|)\,\mathrm{d}k = \sum_{n=1}^{2} G_n(|\xi|,\mu), \tag{30}$$

where

$$G_n(|\xi|,\mu) = (-1)^{n+1}\int_0^\infty \cos\left[|\xi|(t^2+1)(t\mu+(-1)^n)\right]\mathrm{d}t. \tag{31}$$

In this case, only the first integral $G_1$ possesses stationary points. They are

$$t_* = \frac{1 \pm \sqrt{1-3\mu^2}}{3\mu}, \qquad 0 < \mu \le \frac{1}{\sqrt{3}}, \tag{32}$$

which coincide along the line $\mu = \frac{1}{\sqrt{3}}$ $\left(|\xi| = \sqrt{3}|\eta|\right)$. This again motivates us to make use of the uniform stationary phase method, giving

$$G_1(|\xi|,\mu) = \mathrm{Re}\left\{ e^{ip|\xi|} \int_0^\infty e^{i|\xi|\mu\left[\left(t-\frac{1}{3\mu}\right)^3 + 3^{1/3}\mu^{-2/3} q\left(t-\frac{1}{3\mu}\right)\right]} \mathrm{d}t \right\}$$
$$= \frac{2\pi}{\sqrt[3]{3\mu|\xi|}} \cos(p|\xi|)\,\mathrm{Ai}\left(q|\xi|^{2/3}\right), \tag{33}$$

where

$$p = \frac{2(9\mu^2+1)}{27}, \qquad q = \frac{3\mu^2-1}{(3\mu)^{4/3}}, \tag{34}$$

and

$$\mathrm{Ai}(z) = \frac{1}{\pi}\int_0^\infty \cos\left(\frac{t^3}{3} + zt\right) \mathrm{d}t \tag{35}$$

is the Airy function, see Abramowitz and Stegun [15].

The resulting far-field asymptotic expansion for the longitudinal displacements takes the form

$$u_1 \sim -\frac{AP\varepsilon c_{\mathrm{R}}^2 \mathrm{sgn}(\xi)}{c_2^2 bh\sqrt[3]{3|\xi|\mu}} \cos(p|\xi|)\,\mathrm{Ai}\left(q|\xi|^{2/3}\right). \tag{36}$$

Numerical illustrations in Figures 7 and 8, using the scaled displacement

$$U_1 = \frac{bhc_2^2}{APc_R^2\varepsilon} u_1, \tag{37}$$

demonstrate comparisons of the exact solution in equation (29) with its far-field asymptotic approximation (36), depicted, as previously, by solid and dotted lines, respectively.

The calculations for Figure 7 were performed for a fixed value of $|\eta| = 5$, with Figure 8 showing a perpendicular cross-section at $|\xi| = 10$.

It may be observed from Figures 7 and 8 that even though there is no Mach cone in the sub-Rayleigh regime, there is still a region of oscillations associated with $\mu < \frac{1}{\sqrt{3}}$. The period of oscillation decreases as $\mu \to 0$. In the region $\mu > \frac{1}{\sqrt{3}}$ the profile demonstrates exponential decay.

Concluding this section, we present a 3D numerical illustration of the scaled displacement $U_1$ defined in equation (37) over the region $-10 \le \xi \le 0$, $0 \le \eta \le 5$, see Figure 9.

## 5. Concluding remarks

The adapted specialized long-wave model oriented to the surface wave field induced by a moving load on a coated half-space seems to be optimal for analyzing resonant phenomena. It enables the simplification of all the derivations significantly, due to ignoring the contribution of compression and shear bulk waves. In addition, this model provides a more straightforward qualitative insight, including, for example, discussion of the causality principle in the application to a dispersive surface wave.

Scaling, taking into consideration the degeneration characteristics of near-resonant regimes and the small thickness of the coating, was determined. Simple integral solutions of the 2D scaled equation governing the surface motion, were derived for both the sub- and super-Rayleigh cases. The associated wave field over the interior

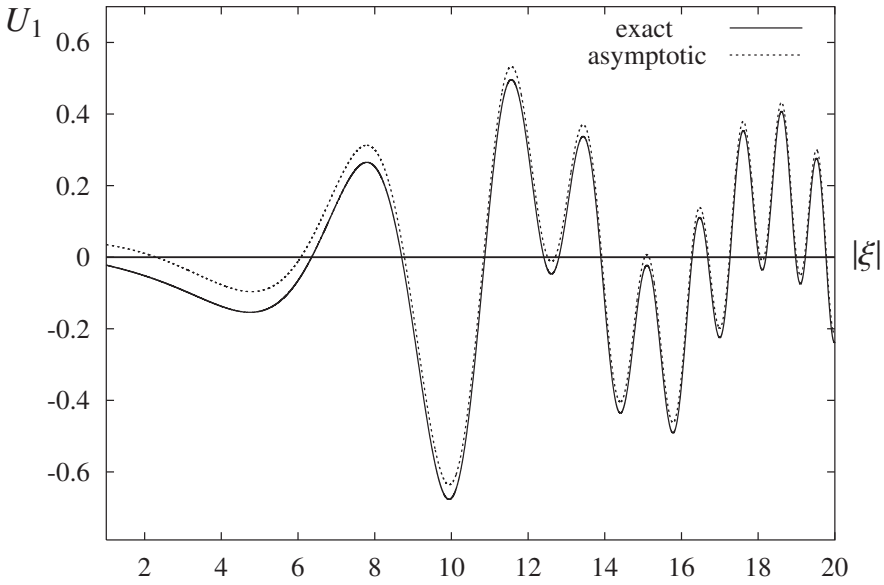


**Figure 7.** Longitudinal cross-section of the sub-Rayleigh displacement profile at $|\eta| = 5$.

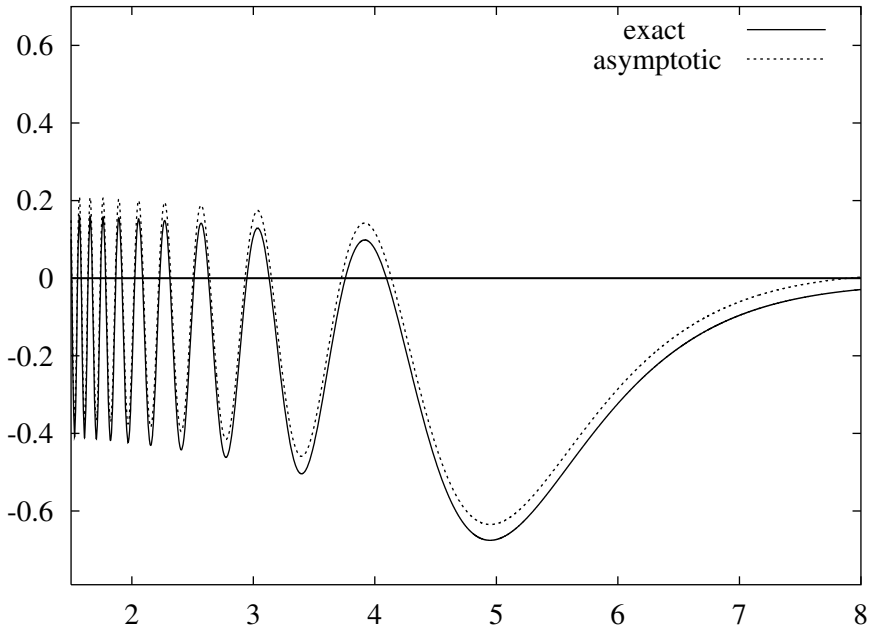


**Figure 8.** Transverse cross-section of the sub-Rayleigh displacement profile $U_1$ at $|\xi| = 10$.

can be relatively easily restored by solving analytically or numerically standard boundary value problems for pseudo-static elliptic equations.

Uniform far-field asymptotic behaviors expressed through the Airy function and Fresnel integrals were established. They can be useful for investigating the transition regions along the surface. For the super-Rayleigh regime, such a region is associated with the contour of a Mach cone. As might be expected, the presence of a coating results in smoothing of the singularities arising in the related problem for an uncoated half-space.

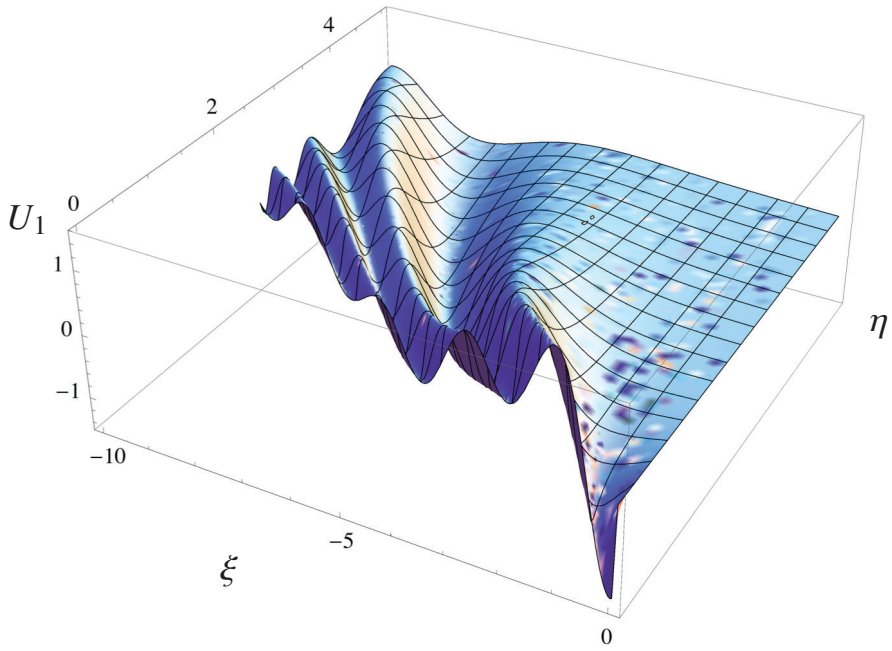


**Figure 9.** A 3D profile of the longitudinal sub-Rayleigh displacement $U_1$ from equation (37).

## Conflict of interest

None declared.

## Acknowledgements

JK and DAP would like to thank Prof CJ Chapman for fruitful discussions regarding the causality principle.

## Funding

The support of Anadolu University (grant number 1306F268) is gratefully acknowledged.

## References

[1] Cao, Y, Xia, H and Li, Z. A semi-analytical/FEM model for predicting ground vibrations induced by high-speed train through continuous girder bridge. *J Mech Sci Technol* 2012; 26: 2485–2496.
[2] Fryba, L. *Vibration of solids and structures under moving loads*. London: Thomas Telford, 1999.
[3] Georgiadis, HG and Lykotrafitis, G. A method based on the Radon transform for three-dimensional elastodynamic problems of moving loads. *J Elast* 2001; 65: 87–129.
[4] Kaplunov, J, Zakharov, A and Prikazchikov, DA. Explicit models for elastic and piezoelastic surface waves. *IMA J Appl Math* 2006; 71: 768–782.
[5] Dai, HH, Kaplunov, J and Prikazchikov, DA. A long-wave model for the surface elastic wave in a coated half-space. *Proc R Soc London, Ser A* 2010; 466: 3097–3116.
[6] Chadwick, P. Surface and interfacial waves of arbitrary form in isotropic media. *J Elast* 1976; 6: 73–80.
[7] Kiselev, AP and Parker, DF. Omni-directional Rayleigh, Stoneley and Scholte waves with general time dependence. *Proc R Soc London, Ser A* 2010; 466: 2241–2258.
[8] Kaplunov, J, Nolde, E and Prikazchikov, DA. A revisit to the moving load problem using an asymptotic model for the Rayleigh wave. *Wave Motion* 2010; 47: 440–451.
[9] Kaplunov, J, Prikazchikov, DA, Erbaş, B and Şahin, O. On a 3D moving load problem for an elastic half space. *Wave Motion* 2013; 50: 1229–1238.
[10] Achenbach, JD, Keshava, SP and Herrmann, G. Moving load on a plate resting on an elastic half-space. *J Appl Mech* 1967; 34: 910–914.

[11] Kalinchuk, VV, Belyankova, TI, Schmid, G and Tosecky, A. Dynamic of layered half space under the action of moving and oscillating load. *Bull South Res Cent RAS* 2005; 1: 3–11.
[12] Kaplunov J, Oblakova, TV and Prikazchikov, DA. Near-resonant regimes of a moving load in the plane-strain problem for a coated elastic half-space. *Mat Model Chislennye Metody* 2014; 1: 57–67.
[13] Shuvalov, AL and Every, AG. On the long-wave onset of dispersion of the surface-wave velocity in coated solids. *Wave Motion* 2008; 45: 857–863.
[14] Borovikov, VA. *Uniform stationary phase method*. London: Institution of Electrical Engineers, 1994.
[15] Abramowitz, M and Stegun, IA. *Handbook of mathematical functions*. New York: Dover Publications, 2012.
[16] Poruchikov, VB. *Methods of the classical theory of elastodynamics*. Berlin: Springer-Verlag, 1992.